MODAL TESTING AND MODEL UPDATING OF A REAL SCALE NUCLEAR FUEL ROD

NAM-GYU PARK, HUINAM RHEE[1*], HOYIK MOON[2], YOUNG-KI JANG, SANG-YOUN JEON and JAE-IK KIM
R&D Center, Korea Nuclear Fuel, P.O. Box 14, Yuseong, Daejeon 305-353, Korea
[1] Mechanical & Aerospace Eng., Sunchon National University, 150 Maegok-dong, Sunchon, 540-742, Korea.
[2] NVS, 291-2 DongRim-Ri, MoHyun-Myun, YongIn city, Kyunggi, Korea.
*Corresponding author. E-mail : hnrhee@sunchon.ac.kr

Received August 28, 2008
Accepted for Publication January 22, 2009

In this paper, modal testing and finite element modeling results to identify the modal parameters of a nuclear fuel rod as well as its cladding tube are discussed. A vertically standing full-size cladding tube and a fuel rod with lead pellets were used in the modal testing. As excessive flow-induced vibration causes a failure in fuel rods, such as fretting wear, the vibration level of fuel rods should be low enough to prevent failure of these components. Because vibration amplitude can be estimated based on the modal parameters, the dynamic characteristics must be determined during the design process. Therefore, finite element models are developed based on the test results. The effect of a lumped mass attached to a cladding tube model was identified during the finite element model optimization process. Unlike a cladding tube model, the density of a fuel rod with pellets cannot be determined in a straightforward manner because pellets do not move in the same phase with the cladding tube motion. The density of a fuel rod with lead pellets was determined by comparing natural frequency ratio between the cladding tube and the rod. Thus, an improved fuel rod finite element model was developed based on the updated cladding tube model and an estimated fuel rod density considering the lead pellets. It is shown that the entire pellet mass does not contribute to the fuel rod dynamics; rather, they are only partially responsible for the fuel rod dynamic behavior.

KEYWORDS : Fuel Assembly, Fuel Rod, Modal Testing, Finite Element Method, Vibration, Natural Frequency, Mode Shape

1. INTRODUCTION

Vibration of a nuclear fuel assembly loaded into a pressurized water reactor (PWR) is unavoidable as it is always exposed to coolant flow which is needed to transfer heat that arises from nuclear fission during the operation of the plant. Random vibration caused by the coolant flow commonly accompanies fretting wear on the cladding tube, and excessive vibration is a major cause of the fuel mechanical failures.

In order to satisfy nuclear safety regulations, the structural strength should be guaranteed for fuel rods. Therefore, it must be verified that the vibration is less than the allowable level and that fluid elastic instability does not occur. Many theoretical and experimental works are devoted to predicting vibration levels using the dynamic properties of a fuel rod (or a similar structure). Premount [1] reported that natural frequencies are dependent on the excitation force level. According to his work, a higher force level induces lower natural frequencies. Knowing that the fluid force acting on a nuclear structure is not deterministic, a turbulent fluid force in cylinder bundles along with the vibration responses of the bundles were predicted using a stochastic approach by Curling and Paidoussis [2]. Calculating vortex-induced vibration, Yamamoto et al. [3] investigated the hydrodynamic interaction between oscillating flexible cylinders and a fluid. General guidelines to prevent tube failure due to an excessive flow in a heat exchanger were introduced [4], and fretting wear damage assessment was covered in their research as well.

Every prediction requires structure information; thus, fuel rod dynamic characteristics such as the mode shapes, modal dampings, and modal frequencies should be investigated when a nuclear fuel is designed so as to predict fuel rod performance against mechanical failures. A series of modal tests of a fuel rod was conducted [5~7], showing several interesting results. In particular a fuel rod of a reduced size with four spans in a water condition was studied experimentally [5], and modal test results on a commercial fuel rod with 8 spans in the horizontal position were published [6,7].

Unlike previous studies [5~7], this paper presents and discusses the modal testing results of a vertically standing

full-size fuel rod with 10 spans and suggests a consistent method of constructing a fuel rod finite element model. A vertical-standing test set-up was prepared to simulate a real situation in which the fuel assemblies are vertically loaded into a nuclear reactor. This paper also compares the modal testing results of a fuel cladding tube as well as a fuel rod with lead pellets to determine to what extent the pellets contribute to the fuel rod kinetics. Depleted uranium can be used for a better realistic simulation, but lead pellets were preferred as procuring uranium or depleted uranium for the test facility is very difficult in practice.

2. MODAL TEST RESULTS OF THE CLADDING TUBE AND THE FUEL ROD

2.1 Test Set-up Overview

The test configuration shown in Fig. 1 consists of a shaker (MB Dynamics MODAL-50A), a shaker hanger, and a vertical test stand with 11 clamps which hold 6 ×6 grid assemblies securely. The test bed is fixed to a concrete wall through 3 I-beams, and the bottom end is fixed to the ground. A force transducer at the tip of a stinger which is linked to the shaker measures the applied force signal,

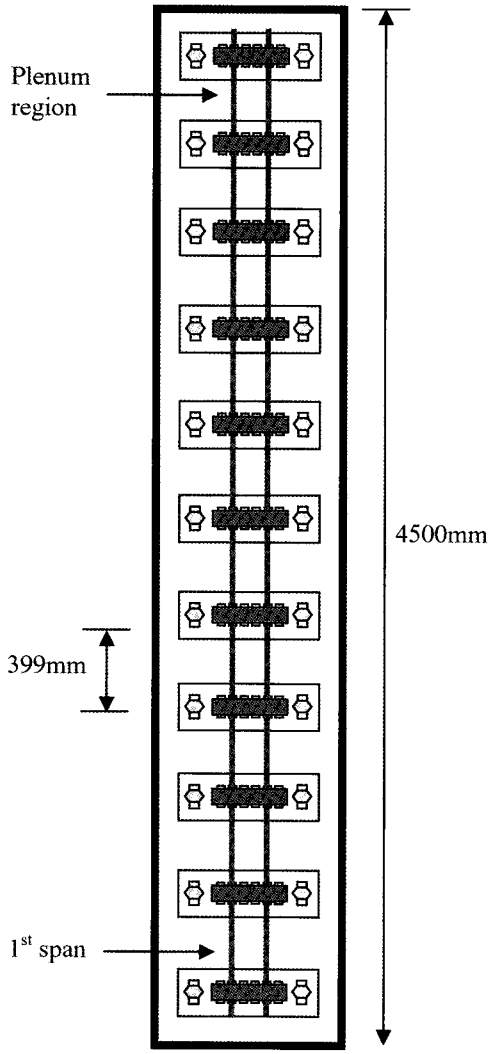

(a) Test stand with the fuel rod and cladding tube supported by 11 grids

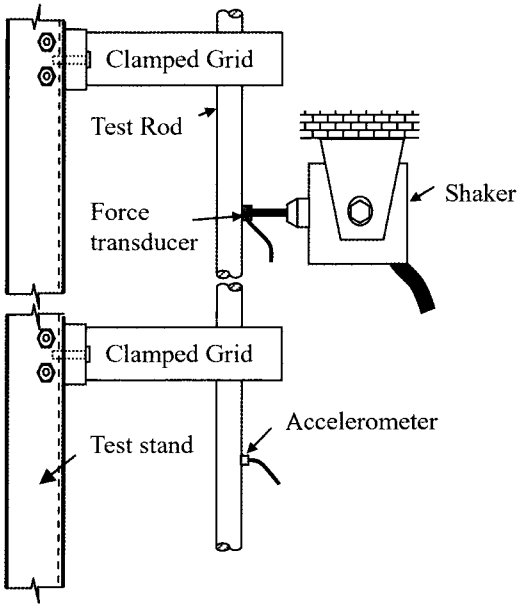

(b) Enlarged view around a shaker attached at the sixth span

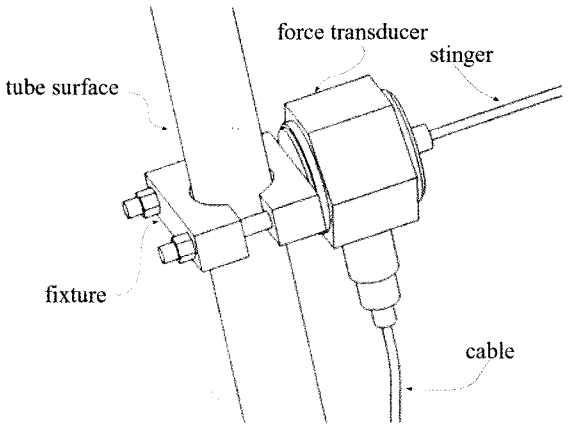

(C) Enlarged side view of the area around the force transducer

Fig. 1. Configuration of the Test Set-up

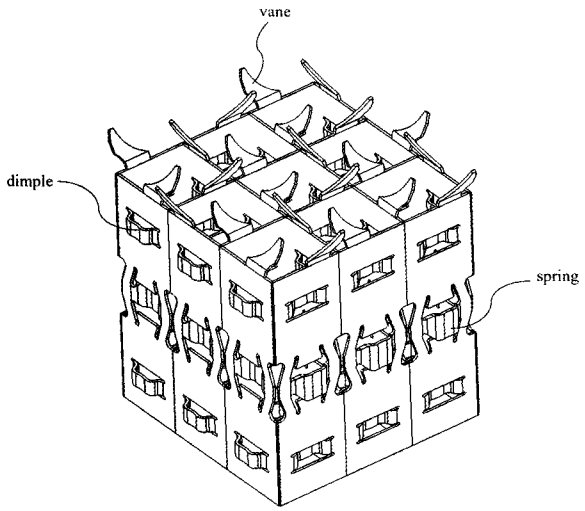

Fig. 2. Configuration of a 3 × 3 Spacer Grid (6 × 6 grid Are Used in the Test)

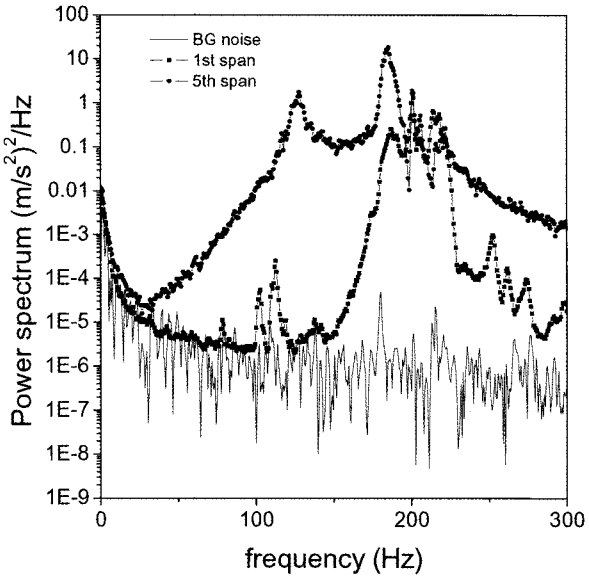

Fig. 3. Measured Noise and Signal Level for the Cladding Tube

and a shaker placed in the middle of the sixth span is fixed to a rigid wall, as shown in Fig. 1(b). Particularly, as fuel rod surface is round whereas the force transducer top and bottom surfaces are flat, a fixture to provide a flat surface for the rod is necessary to join the force transducer to the structure. Fig. 1(C) shows the assembled set-up configuration of the force transducer.

Two types of fuel rods were inserted through the grid structures in the test bed. While the left sample in Fig. 1(a) consists of a cladding tube along with end plugs, the right sample also contains lead pellets. Axial movement of the lead pellets in the fuel rod is tightly restricted by a coil spring placed in the plenum region that compresses the pellets. The entire length of the fuel rod is approximately 4.1 m, and the outer diameter is 9.5 mm.

Three ICP® accelerometers (PCB) were utilized, and accelerations of three points on the fuel rod were measured simultaneously. The accelerometers were placed at every 1/4, 2/4, and 3/4 location along the fuel rod at each span. Unlike the force transducer, which requires the fixture, the accelerometers are directly attached to the rod with wax. The accelerometers used in this study are minuscule, with each weighing only 2 g; however, a thin layer of the rod surface at which the accelerometer is placed was removed to assure a secure attachment. Signals were measured and analyzed using LMS Test.Lab.

Fig. 2 shows a spacer gird which consists of an arrangement of interlocked straps, with springs and dimples formed within the straps, for gripping and holding the fuel rods in the proper position within the fuel assembly structure. Nine mid-grids, one top and one bottom grid are fixed with 11 clamps to the test bed, and one fuel rod and one cladding tube are loaded through the grids.

To identify the signal-to-noise ratio (SNR), the

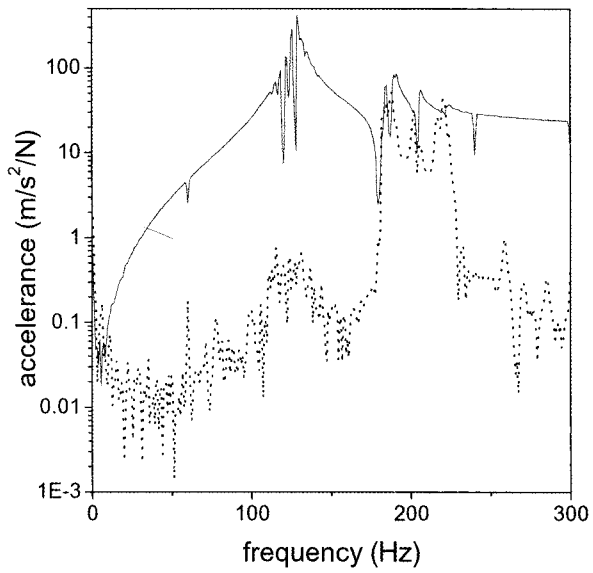

Fig. 4. Measured Cladding Tube Frequency Response Function (Solid Line: Shaker Position; Dotted Line: Bottom Position)

background noise and power spectra were measured as shown in Fig. 3. As the measurement point is located away from the shaker location, the level of noise is comparable to the level of tube response in all frequency ranges. Considering that the shaker is fixed at the sixth span, a detrimental SNR value is predictable, as the measurement location is far away from the excitation position. Fig. 4 shows measured frequency response functions at the

Table 1. Measured Natural Frequencies (Hz)

Mode number	1	2	3	4	5
Cladding tube (Ω_t)	125	181	193	203	213
Fuel rod (Ω_r)	83	95	103	108	113
$(\Omega_t/\Omega_r)^2$	2.26	3.59	3.29	3.6	3.85

Table 2. Material and Sectional Properties of the Cladding Tube

Young's modulus (Pa)	density (kg/m^3)	radius of gyration (m)	cross-section area (m^2)
9.831E10	6.56E3	3.162E-3	1.603E-5

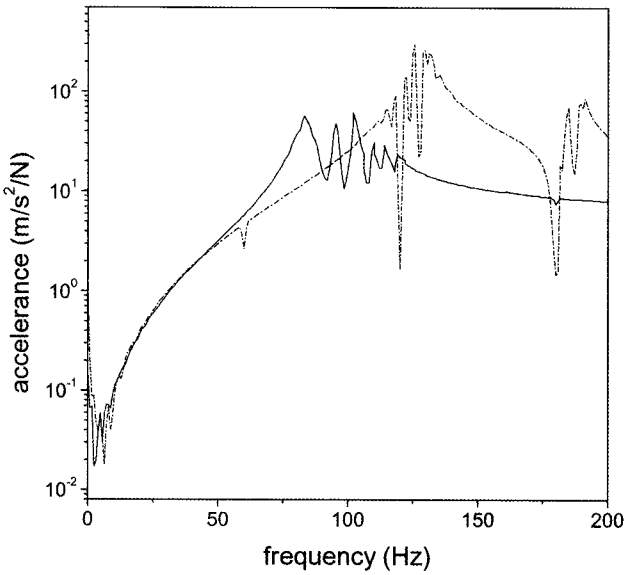

Fig. 5. Measured Frequency Response Functions. Solid Line: Fuel Rod; Dash Dotted Line: Cladding Tube

shaker position and at the bottom point. As with the SNR, the signal level in the shaker position is considerably larger than that in the bottom position, apart from the narrow band. It is likely that the friction between the fuel rod and spacer grids which dissipate the vibration energy mainly causes the bad SNR when a signal is measured relatively far from the shaker position.

2.2 Test Results

A random force signal was applied to a shaker placed in the middle point of the sixth span and the frequency response functions of a cladding tube were measured. Separate tests of a fuel rod were also performed. Table 1 shows the measured natural frequencies of the cladding tube and of the rod, and the measured frequency response functions are delineated in Fig. 5. The natural frequency difference is clearly shown in Table 1 and Fig. 5, while the mode shapes do not differ significantly, as shown in Fig. 6, which shows the first four modes of the cladding tube and the rod. The lower natural frequencies of the fuel rod are due to the lead pellets.

The bending wave propagation speed in a beam is expressed as follows [8]:

$$c_b = \sqrt{\omega} \cdot \sqrt[4]{E\kappa^2 / \rho} \tag{1}$$

Here, κ is the radius of the gyration of the cross-sectional area of the cladding tube. E, ω, and ρ denote the Young's modulus, circular frequency, and the fuel rod or tube density, respectively. It is possible to calculate the wavelength of the first-mode frequency (125Hz) of the cladding tube using Eq. (1) and material properties listed in Table 2. This result is 784 mm. Considering that one span length is close to 399 mm, the wavelength approximately corresponds to the length of two spans. This result shows why the mode has nodal points in the spacer grids. On the other hand, the wavelength in the other mode is less than that of the first mode. For example, the wavelength of the second mode is close to 650 mm. If the frequency is increased, the wavelength decreases because it is inversely proportional to the frequency. In addition, a standing wave cannot be maintained owing to the structural damping, implying that the nodal points in each mode can vary. Considering that the dimple-to-dimple distance in each grid is approximately 30 mm, a varying nodal point range is feasible within the measured frequency band.

The same method can be applied to the fuel rod, but the fuel rod density should be identified. Though the

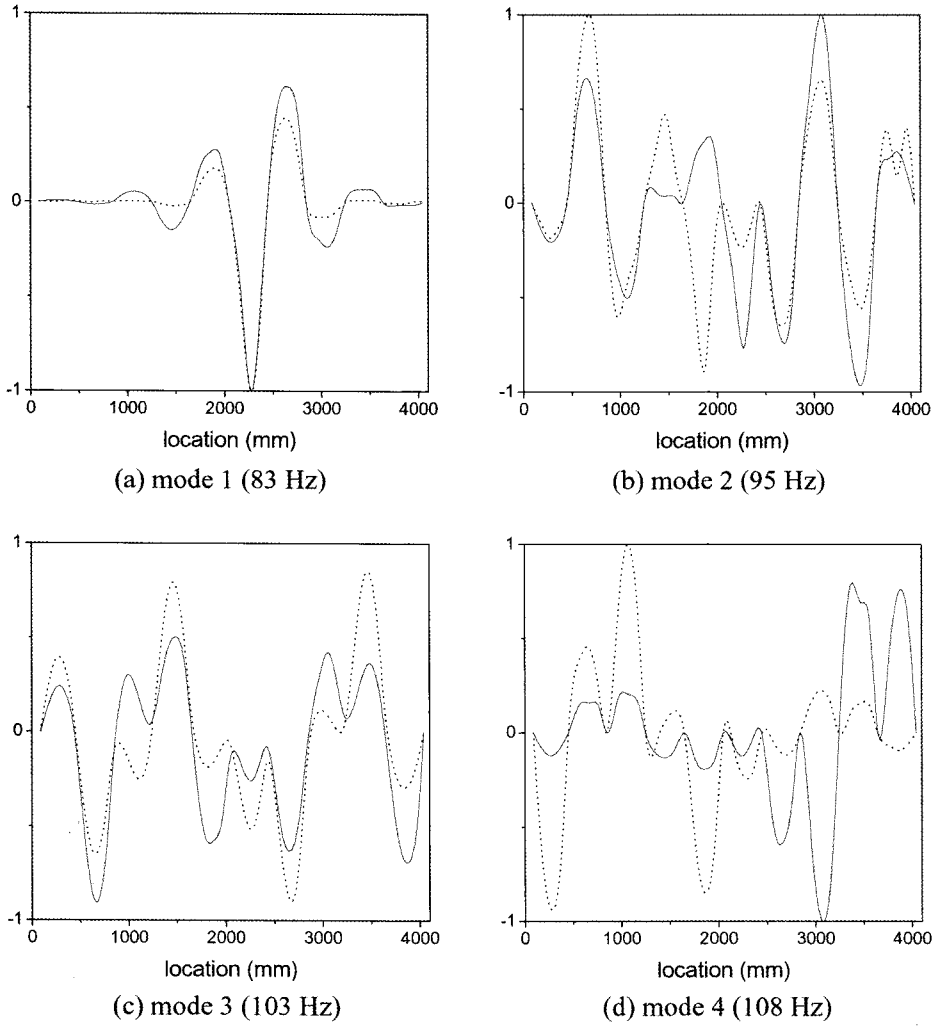

Fig. 6. Experimental Modes Normalized to the Maximum (Solid line: Rod; Dotted Line: Tube). The Frequencies in the Parenthesis Denote the Measured Natural Frequencies in the Fuel Rod

pellet axial movement is constrained with the plenum spring, the pellets can rattle inside the cladding tube considering the gap between the tube and the pellet. A useful approximate estimation methodology for the fuel rod mass is given below.

3. FINITE ELEMENT MODEL GENERATION AND ITS IMPROVEMENT

3.1 Lumped Mass Identification

Cladding tube mechanical properties such as the density and Young's modulus can easily be determined. The spring stiffness in the cell also can be estimated based on a cell stiffness test. Although the grid structural geometry is very complex, the spring and dimple in each cell can be considered as linear springs for low-amplitude vibration. To predict the dynamic behavior of a fuel rod, it is convenient and reasonable to assume that every spring in the cell maintains constant contact with the fuel rod. When the gap between the tube and spring is large enough, this assumption may no longer be valid. However, considering manufacturing tolerance issues such as grid misalignments, a perfectly gapped condition cannot be maintained as fuel rods are not perfectly straight and the spring height in each cell is not constant. This implies that fuel rods loaded in grids can be slightly skewed; it is considered that the above assumption is valid when the gap is less than 0.254 mm (0.010 inch) based on fuel assembly tests in a reactor simulator.

A schematic of a finite element (FE) cladding tube model developed using MATLAB is shown in Fig. 7. This consists of 119 nodes and 118 beam elements. As the dynamic characteristics of an initial FE model usually

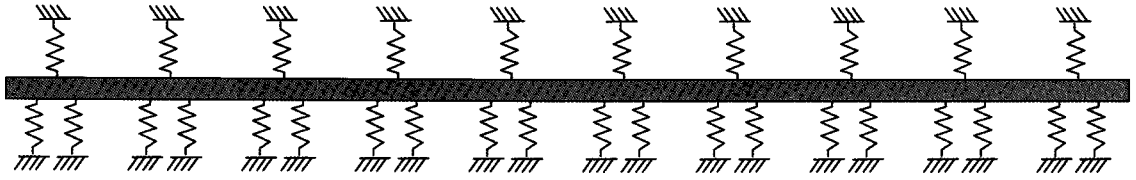

Fig. 7. Simplified Model of the Fuel Rod Loaded in Grids

deviate from the measured values, FE model updating should be done. The FE model can be improved by updating a number of uncertain design parameters. A lumped mass attached to the force sensor position on the fuel rod was chosen as an uncertain parameter in this study because the force transducer including the fixture, the stinger, and the shaker dynamic mass is much larger compared to a slender fuel rod. As the accelerometers are tiny and because only three accelerometers are discretely attached in a span, their masses were excluded. The spring stiffness in each cell could be another uncertain parameter, but the spring stiffness is not a governing parameter because the modal displacements near the spacer grids are close to zero. In more detail, the sensitivity of the natural frequency with respect to the spring stiffness can be written as [11]

$$\Delta\lambda_i \approx \Delta k_j \left(\phi_i^j\right)^2, \tag{2}$$

where λ_i is the i-th eigenvalue, the square of the modal frequency; Δk_j is the variation of the j-th spring element; and ϕ_i^j is the j-th element of the i-th mode shape vector. If ϕ_i^j is nearly zero, the natural frequency variation will be negligible regardless of the stiffness change. Given that every mode from the modal testing shows mostly nodal points at the spacer gird locations, the stiffness is not considered as an important parameter in this case compared to the influence of the lumped mass, despite the fact that the spring stiffness may be a significant parameter in an actual case. Minimization of the natural frequency difference was done to obtain the improved FE model. Consequently, the optimization problem can be defined as follows:

$$\min \frac{1}{2} \Lambda(p)^T \Lambda(p) \tag{3}$$

Here, p denotes the lumped mass and $\Lambda \in R^N$. The residual function, $\Lambda : R \rightarrow R^N$, which is nonlinear in terms of p, denotes the difference vector between the target and the current natural frequencies. When the target natural frequencies are denoted as f^t, then $\Lambda = [(f_1 - f_1^t) \ldots (f_N - f_N^t)]^T$. N is the number of target natural frequencies of the cladding tube, which comes from the modal testing.

This optimization problem requires a solution technique for nonlinear optimization, in which an iterative process is generally indispensable. The solution of Eq. (3) is obtained without difficulty by applying Gauss-Newton's method iteratively. Typically, the solution of each iteration is

$$\{p\}_{i+1} = \{p\}_i - \left(J(\{p\}_i)^T J(\{p\}_i)\right)^{-1} J(\{p\}_i)^T \Lambda(\{p\}_i) \tag{4}$$

where J indicates a Jacobian, a natural frequency sensitivity vector with respect to the mass. As the Jacobian of Eq. (4) is not always well conditioned, Gauss-Newton's method is not considered to be globally convergent. Thus, various modified Newtonian methods have been developed for this type of problem. The *Levenberg-Marquardt* method [9] is applied in the present study. The optimization process was completed using MATLAB.

The lumped mass as a function of the iteration number is shown in Fig. 8. The identified mass is nearly 28 g, which is mainly due to the force transducer considering

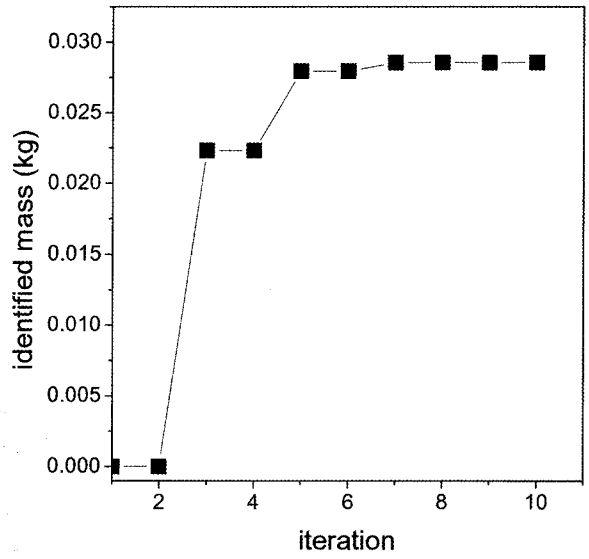

Fig. 8. Lumped Mass Updating Results

Table 3. Initial and Final Natural Frequencies of the Cladding Tube (Hz)

Mode number		1	2	3	4	5	6	7
FE Model	Initial	165	169	178	189	202	-	217
	final	124	169	171	189	192	-	215
Measured		125	-	-	181	193	203	213
MAC (%) FE final vs. measured		97	-	-	19	89	-	24

Table 4. The First Natural Frequencies in Cladding Tubes with Limited Spans

Number of total spans	1	2	3	4
The first natural frequency (Hz)	185	174	170	168

that the force sensor weight is 22.7 g. The deviation between the identified mass and the given force transducer mass explains that the fixture, the stinger weight, and the shaker dynamic mass can contribute to the lumped mass effect. Fairly considerable updating results with only the lumped mass show that the lumped mass is the major uncertain parameter in this case.

Table 3 shows the natural frequencies of the cladding tube initial and updated FE models. The second and third natural frequencies of the tube model do not appear in the measurement in Table 3. These missing modes are thought to be locally generated modes of the cladding tube model, and the natural frequencies of the tube with the limited number of spans in Table 4 are in reality quite close to the second and third natural frequencies of the cladding tube model. This signifies that the second and the third modes can be local modes.

While the second and third modes were not obtained in the modal testing, the sixth mode from the test could not be found in the FE model. When the measured mode shape at 203 Hz was compared to the FE mode at 192 Hz and the measured mode at 193 Hz, it was found that the mode at 203 Hz was roughly similar to both, as shown in Fig. 9. In addition, the MAC (Mode Assurance Criterion) value, which measures the degree of mode shape similarity [12] between the measured mode at 203 Hz and the FE mode at 192 Hz, was determined to be 40%. Therefore, it is thought that the mode at 203 Hz, not shown in the FE model, is a degenerated one relative to the other mode.

The MAC value between the final FE mode and measured mode is also listed in Table 3. This table shows that the two mode sets are very close whereas the other two sets are not as similar. Fig. 10 shows the two mode sets with low MAC values. In the first case, the phase of the measured mode differs from that of the analytic mode; half of the wave phase is opposite. On the other hand, it

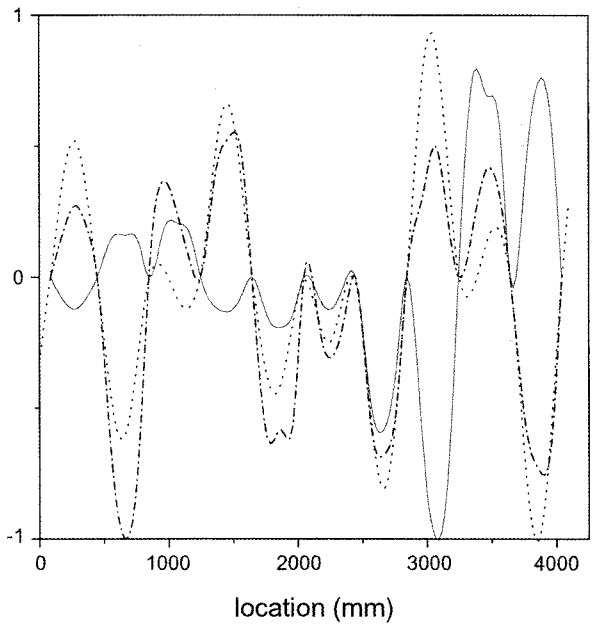

Fig. 9. Measured Modes vs. Predicted Mode (Solid Line: Measured at 203 Hz, Dotted Line: FE Mode at 192 Hz, Dash Dotted Line: Measured at 193 Hz)

is clear that, besides the phase, the amplitudes are different in the second case. It is thought that a noise-contaminated signal induces distorted modes during signal processing.

3.2 Fuel Rod Density Identification

As mentioned earlier, lead pellets instead of uranium pellets were loaded into one cladding tube as uranium pellets are radioactive and therefore difficult to obtain. The diameter of the lead pellets was determined to provide

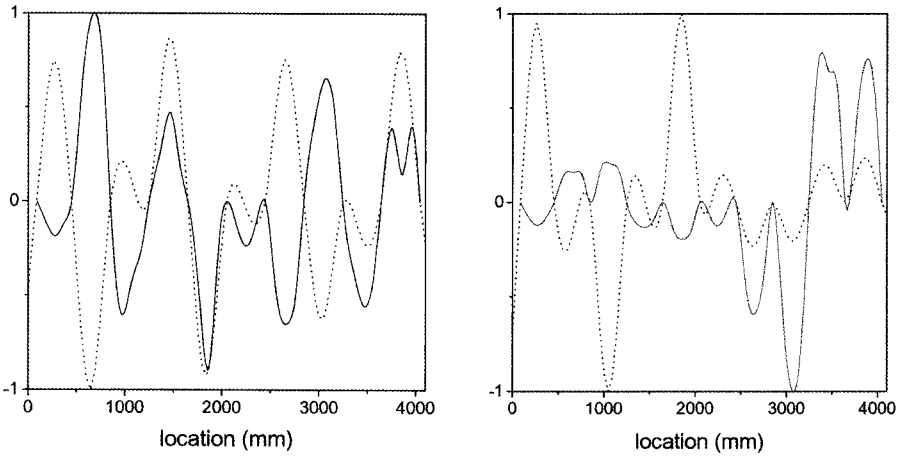

(a) Case 1 (181 Hz) (b) Case 2 (213 Hz)

Fig. 10. Cladding Tube Mode Sets with a Low MAC Value (Solid Line: Experiment, Dotted Line: FE Model)

Table 5. Measured and Predicted Natural Frequencies (Hz)

	1st	2nd	3rd	4th	5th
Measured	83	95	103	108	113
Predicted 1 *	64	69	72	78	84
Predicted 2 ‡	91	103	107	116	125
Predicted 3 †	83	94	97	105	113

* : $\rho_r=(A_t\rho_t+A_p\rho_p)/A_t$; chere A_t denotes the tube cross-section area, A_p and ρ_p refer to the lead pellet cross-section area and density
‡ : $\rho_r=\rho_t+\rho_p$
† : $\rho_r=3.32\rho_t$

approximately the same weight as uranium pellets. The nominal inner diameter of the cladding tube was 8.35 mm, while the pellet diameter was approximately 7.78 mm. Hence, the gap between the pellets and the tube was close to 0.57 mm.

It is assumed that the pellets scarcely contributed to the bending rigidity of the fuel rod due to the gap between the tube and the pellets during the modal test. Therefore, it is reasonable to assume that the pellets contributed only to the mass and not to the stiffness of the FE model. Therefore, the natural frequency ratio between the fuel rod and the cladding tube is expressed as follows [10]:

$$\frac{\Omega_t}{\Omega_r}=\sqrt{\frac{\rho_r}{\rho_t}} \tag{5}$$

Here, Ω and ρ indicate the natural frequency and density, and the subscripts 'r' and 't' denote the rod and the tube, respectively. According to Eq. (5), once the natural frequency ratios and cladding tube density are known, the equivalent fuel rod density can be calculated.

Natural frequency ratios based on experimental results are given in Table 1. They are not constant for each mode. The mean value, 3.32, was used to estimate the fuel rod density. When the density of the FE model is used as the linear sum (17.36E3 kg/m^3) or the area-weighted sum of the cladding tube and pellet densities (40.1E3 kg/m^3), the natural frequencies of the FE model are different from the measured values, as shown in Table 5. On the other hand, when the adjusted density is used for the FE model based on Eq. (5), deviation of the frequency is reduced significantly, as shown in Table 5. Fig. 11 shows the measured and predicted frequency responses. The updated FE model generates much more consistent results with the measurement.

It is possible to calculate the wavelength at the first-mode frequency (83Hz) using Eq. (1). This was found to be 713 mm, which is shorter than that of the cladding tube. The discrepancy may be due to an estimation error of the fuel rod density or to unidentified nonlinearities. Usually, high-frequency vibration is expected in a reactor

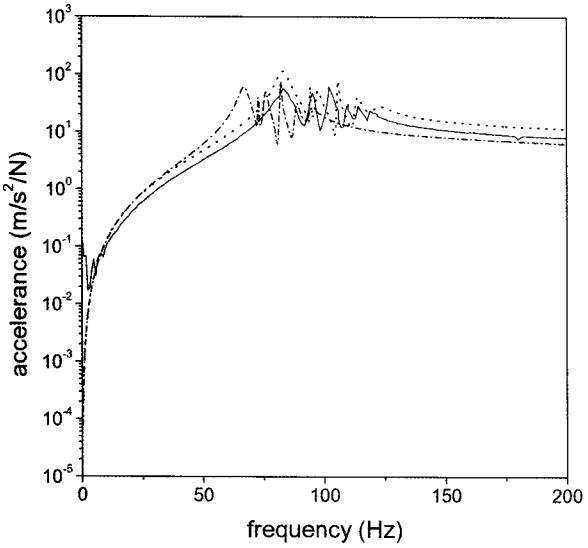

Fig. 11. Measured and Predicted Frequency Response Functions. Solid Line: Measured; Dotted Line: Density Adjusted; Dash Dotted Line: Summation of the Tube and Pellet Densities

condition; thus, lateral motion of the pellets in the rod does not occur in the same phase. All pellets, therefore, cannot contribute to the kinetic energy simultaneously when the rod is exposed to a turbulent flow.

4. CONCLUSION

A fuel rod with pellets is highly nonlinear due to the interaction between the pellets and the cladding tube. In this paper, modal testing was performed for a commercial PWR nuclear cladding tube and a rod with lead pellets using a vertically standing test stand to simulate actual operation conditions. The fuel rod and the tube were loaded into 11 6×6 spacer grid structures along the axial length, and the modal parameters were identified through modal testing. It was found that the friction between the fuel rod and the spacer grids which dissipates the vibration energy mainly causes the detrimental SNR value when a signal is measured at a position far from the shaker position. Additionally, this makes it difficult to estimate mode shapes where the measurement position is far away from the shaker position.

A cladding tube finite element model was initially built based on the nominal design data. It was then updated using optimization techniques to minimize discrepancies between the test and the analysis results. It was found that the effect of the lumped mass modeled as an added mass at the excitation location severely changes the dynamic characteristics of the cladding tube and that a point mass added to the model greatly improved the analysis model. To construct a reliable FE model of the fuel rod with the pellets, the density of the rod was estimated based on the test results. It is clearly shown that the results of the FE model with the equivalent density shows consistent dynamic characteristics compared to those of the test data.

In the course of this work, a number of uncertain parameters related to the cladding tube and fuel rod with pellets were identified, and significant improvement of the FE models was achieved. The difficulty with the modal testing was largely due to the friction between the rod and the spacer grids. More elaborate modal testing of a fuel rod considering highly nonlinear characteristics should be performed in the future. In addition, as the fuel rod structure is very slender and long, a multipoint excitation test should be considered to acquire better results.

ACKNOWLEDGEMENTS

This work was funded by the Korea Ministry of Knowledge Economy (R-2005-1-391 and R-2006-1-243-2). The authors express their gratitude. The corresponding (second) author also wants to express gratitude for the support by the NURI project of the Ministry of Education & Human Resources Development, Korea in 2007~2009 and for that by the Research Foundation of Engineering College of Sunchon National University.

REFERENCES

[1] A. Premount, "On the Vibrational Behavior of Pressurized Water Reactor Fuel Rods," Nuclear Technology, Vol. 58, pp. 483~491 (1982).

[2] LI.R. Curling, M.P. Paidoussis, "Analysis for Random Flow-Induced Vibration of Cylindrical Structures Subjected to Turbulent Axial Flow," Journal of Sound and Vibration, Vol. 264, pp. 795~833 (2003).

[3] D.T. Yamamoto, J.R. Meneghini, F. Saltara, R.A. Fregonesi, J.A. Ferrari Jr., "Numerical simulation of Vortex-Induced Vibration on Flexible Cylinders," Journal of Fluids and Structures, Vol. 19, pp. 467~489 (2004).

[4] M.J. Pettigrew, C.E. Taylor, "Vibration Analysis of Shell-and-tube Heat Exchangers: An Overview-Part 2: Vibration Response, Fretting Wear, Guidelines," J. Fluids and Structures, Vol. 18, pp. 485-500 (2003)

[5] H.S. Kang, K.N. Song, H.K. Kim, K.H. Yoon, Y.H. Hung, "Verification Test and Model Updating for a Nuclear Fuel Rod with Its Supporting Structure," Journal of the Korea Nuclear Society, Vol. 33, No.1, pp. 73~82 (2001).

[6] M.H. Choi, H.S. Kang, K.H. Yoon, K.N. Song, "Vibration Analysis of a Dummy Fuel Rod Continuously Supported by Spacer Grids," Nuclear Engineering and Design, Vol. 232, pp. 185~196 (2004).

[7] M.H. Choi, H.S. Kang, K.H. Yoon, K.N. Song, "An Experimental Study on the Vibration of the PWR Fuel Rod Supported by the Side-slotted Plate Springs," Journal of the Korea Society Noise and Vibration Engineering, Vol. 13, No. 10, pp. 798~804 (2003).

[8] L.E. Kinsler, A.R. Frey, A.B. Coppens, J.V. Sanders, *Fundamentals of Acoustics*, John Wiley & Sons (1982).

[9] J.E. Dennis, R.B. Schnabel, *Numerical Methods for*

Unconstrained Optimization and Nonlinear Equations, Prentice Hall (1983).

[10] N.G. Park, H.N. Rhee, J.K. Park, S.Y. Jeon, H.K. Kim, "Indirect Estimation Method of Turbulence Induced Fluid Force Spectrum Acting on a Fuel Rod," Nuclear Engineering and Design, Vol. 239, pp.1237~1245 (2009).

[11] M. Friswell, J.E. Mottershead, *Finite Element Model Updating in Structural Dynamics*, Springer (1995).

[12] W. Heylen, S. Lammens, P. Sas, *Modal Analysis Theory and Testing*, Katholieke Universiteit Leuven (1997).